Title
σ-Aromaticity in polyhydride complexes of Ru, Ir, Os, and Pt

Journal
Physical Chemistry Chemical Physics, 18(17)

ISSN
0956-5000

Authors
Jimenez-Izal, Elisa
Alexandrova, Anastassia N

Publication Date
2016-04-28

DOI
10.1039/c5cp04330a

Peer reviewed

PCCP

PAPER

View Article Online
View Journal

Cite this: DOI: 10.1039/c5cp04330a

σ-Aromaticity in polyhydride complexes of Ru, Ir, Os, and Pt†

Elisa Jimenez-Izal[a] and Anastassia N. Alexandrova*[ab]

Received 23rd July 2015,
Accepted 17th September 2015

DOI: 10.1039/c5cp04330a

www.rsc.org/pccp

Transition-metal hydrides represent a unique class of compounds, which are essential for catalysis, organic synthesis, and hydrogen storage. In this work we study $IrH_5(PPh_3)_2$, $(RuH_5(P^iPr_3)_2)^-$, $(OsH_5(P^iPr_3)_2)^-$, and $OsH_4(PPhMe_2)_3$ polyhydride complexes, inspired by the recent discovery of the σ-aromatic $PtZnH_5^-$ cluster anion. The distinctive feature of these molecules is that, like in the $PtZnH_5^-$ cluster, the metal is five-fold coordinated in-plane, and holds additional ligands at the axial positions. This work shows that the unusual coordination in these compounds indeed can be explained by σ-aromaticity in the pentagonal arrangement, stabilized by the atomic orbitals on the metal. Based on this newly elucidated bonding principle, we additionally propose a new family of polyhydrides that display a uniquely high coordination. We also report the first indications of how aromaticity may impact the reactivity of these molecules.

1 Introduction

Aromaticity is a very important concept in the contemporary chemistry: the particular electronic structure of aromatic systems, where electrons are delocalized, explains their large energetic stabilization and low reactivity. Since π-aromaticity was proposed to understand the structure and inertness of benzene, this property has been found in a variety of molecules, including inorganic compounds. It was shown, for instance, that many all-metal aromatic systems display not only π-, but also σ- and δ-aromaticity.[1–8] Regarding the σ-aromaticity, it occurs when σ electrons are delocalized over n atoms ($n > 2$). The smallest compound possessing this particular property is the H_3^+ cluster.[9] Also the H_5^- pentagonal cluster was proposed to be σ-aromatic,[10] though it was found to be a saddle point in the potential energy surface. In this vein, recently, a joint experimental and theoretical work studied the $PtZnH_5^-$ cluster anion.[11] This molecule has a singular planar pentagonal pyramidal coordination for platinum. The authors found that the H_5 cycle is σ-aromatic, and the quasi-planar minimum is stabilized through the involvement of the Pt 5d orbitals (AOs). This σ-aromaticity confers the unusual stability on the hydride. This finding is important due to the substantial presence of transition-metal hydrides in synthetic and structural inorganic and organometallic chemistry.[12–14] Moreover, it should be pointed out that hydride complexes play an essential role in many catalytic cycles, where they have either been used as catalysts or invoked as key intermediates.[15,16] Aromaticity in general is associated with high symmetry, stability, and specific reactivity. Therefore, the stability of transition-metal hydride complexes might have an important repercussion in the kinetics of the catalytic reactions.

The $PtZnH_5^-$ cluster, where the special coordination was first linked to aromaticity, was obtained only in the gas phase. However, there are known compounds synthesized in solution, where a similar, anomalous coordination of transition metals can be found. Among the transition-metal polyhydrides reported in the literature,[17,18] *i.e.*, complexes containing four to nine hydride ligands covalently bound to the metal, four species attracted our attention: $IrH_5(PPh_3)_2$,[19] $(RuH_5(P^iPr_3)_2)^-$,[20] $(OsH_5(P^iPr_3)_2)^-$,[20,21] and $OsH_4(PPhMe_2)_3$.[22] The distinctive feature of these molecules is that, like in the previously mentioned $PtZnH_5^-$ cluster, the metal has a five coordinated arrangement in-plane, along with additional ligands at the axial positions. It is typical for these metals to adopt the square planar coordination, but not five-fold planar. It might be speculated that the full set of d-AOs has an overall spherical symmetry, and thus no preferred directionality of the ligands other than dictated by their steric repulsion. However, this possibility can be ruled out through the examination of the diverse set of complexes considered here, all of which feature the planar pentagonal arrangements of hydrogens, regardless of the axial ligands. Hence, we decided to find out if the stability of these compounds is also governed by σ-aromaticity, and if so – then what the implications on reactivity might be. Based on the reported findings, we will furthermore propose a new family of transition-metal hydrides, whose structures and stabilities are governed by the same bonding phenomenon.

[a] Department of Chemistry and Biochemistry, University of California, Los Angeles, CA 90095-1569, USA. E-mail: ana@chem.ucla.edu
[b] California NanoSystems Institute, University of California, Los Angeles, CA 90095-1569, USA

† Electronic supplementary information (ESI) available. See DOI: 10.1039/c5cp04330a

2 Methods

Geometries were fully optimized using the PBE0[23–25] functional within the Kohn–Sham implementation[26] of density functional theory[27] using the Gaussian09 program.[28] Open-shell structures considered in this work have a doublet spin-state and they were studied using the unrestricted form of the PBE0 functional (UPBE0). The optimized ground state structures were confirmed to be true minima by harmonic frequency calculations obtained by analytical differentiation of gradients. The basis set used throughout was of the triple-ζ quality from Weigend and Ahlrichs denoted as def2-TZVP[29] including a 60-electron relativistic effective core potential for Pt, Os, and Ir. The natural bond orbital (NBO) analysis[30] was performed at the same theoretical level to extract the atomic charges and to determine possible resonance structures and weights using natural resonance theory.[31,32] In addition, chemical bonding analysis was performed using the adaptive natural density partitioning (AdNDP) method.[33] The AdNDP method is a localization scheme for valence electrons that recover both Lewis bonding elements (1c–2e lone pairs and 2c–2e classical covalent bonds), and delocalized bonding elements associated with multi-center-2e bonding up to the maximal number of atoms in the system. The latter bonding elements can be found in aromatic and sometimes also antiaromatic clusters and molecules. Thus, AdNDP achieves a seamless description of systems featuring both localized and delocalized bonding. The AdNDP analysis was done at the PBE0/LANL2DZ level of theory.[23–25]

3 Results

This section is divided into three parts. In Section 3.1, we analyze the $IrH_5(PPh_3)_2$, $(RuH_5(P^iPr_3)_2)^-$, and $(OsH_5(P^iPr_3)_2)^-$ complex hydrides, and probe the changes in the found σ-aromatic arrangement upon changing the ligands or the transition-metal atom. In Section 3.2, the analogous procedure is applied to the $OsH_4(PPhMe_2)_3$ molecule. In Section 3.3 we analyze whether or not Os and Ir can form similar compounds to the σ-aromatic $PtZnH_5^-$ cluster anion.

3.1 $IrH_5(PPh_3)_2$, $(RuH_5(P^iPr_3)_2)^-$, $(OsH_5(P^iPr_3)_2)^-$ and related hydrides of Pt

In Fig. 1A the optimized structure of the $IrH_5(PPh_3)_2$ molecule is shown. Iridium has a five coordinated arrangement in-plane, being bonded to 5 hydrogen atoms. At the axial positions the metal is bonded to two triphenylphosphine ligands. In order to check if the stabilization of this uncommon geometry is due to the σ-aromaticity, as in the case of the $PtZnH_5^-$ cluster anion, we first analyzed the molecular orbitals (MOs). For the sake of clarity only valence MOs where hydrogens are involved are shown in Fig. 1A (the full set of valence MOs can be found in the ESI†). The quasi-degenerate HOMO−1 and HOMO−2 orbitals (energy difference of 0.33 kcal mol^{-1}) are formed by the five 1s AOs of the hydrogens, with a small contribution of iridium's 6p AOs. These are partially bonding, delocalized σ-MOs. The HOMO−38 MO is a completely bonding σ-MO, made of 1s AOs of hydrogens, slightly mixed with the 6s AO on iridium. These three MOs are the only ones that involve significant contributions from Hs; populated by 6 electrons, they make the molecule σ-aromatic, according to Hückel's electron counting rule ($4n + 2$ with $n = 1$). The analogy with the hypothesized H_5^- system is clear. The main difference, however, is that the pentagonal H_5^- cluster is unstable, even though it has the appropriate σ-aromatic arrangement.[10] Thus, this σ-aromatic H_5^- cycle is stabilized through the support of the central iridium atom. Moreover, the $(IrH_5(PPh_3)_2)^-$ anion is also stable and possesses the same aromatic arrangement as its neutral molecule. Interestingly the removal of the ligands leads to a stable IrH_5^- cluster that has the D_{5h} symmetry. The bonding pattern in this species is also σ-aromatic according to the MO-analysis.

To gain insight into the electronic structure of the molecule, we used the AdNDP method. AdNDP, nevertheless, has a limitation on the size of the density matrix that can be managed. Therefore, we performed the AdDNP analysis on the neutral IrH_5 molecule, the smallest entity representative of the studied molecule. This molecule has a $D_{5h}(^1A')$ symmetry and it is a minimum in the potential energy surface. Its MOs are shown in the ESI,† and the ones involving hydrogens have the same shape/composition. The AdNDP procedure produced two possible localized bonding pictures. The first one consists of five covalent, classical 2c–2e bonds between Ir and hydrogens (see Fig. 2A). The occupation numbers for these bonds are bigger than 1.99*e*. This structure may seem to be unusual from the standpoint of the coordination chemistry of Ir, if to think of the orientations of the d-AOs on the atom. However, having a charge of −1.54, Ir is close to a d^{10} configuration, and the fully populated d-AOs jointly have the *K*-symmetry, thus producing no particularly preferred directionality of the metal–ligand bonds. For the second bonding picture, we took into account that the MO analysis shows 8 lone pairs of valence electrons on Ir, and extracted these electrons from the density matrix setting up an occupation number of *ca.* 1.5 electrons. The rest of the density matrix then localizes the H_5 σ-aromatic arrangement, with three localized AdNDP orbitals, being identical to the MOs of the $IrH_5(PPh_3)_2$ molecule (see Fig. 2B). The occupation numbers in this case are bigger than 1.99*e*. The co-existence of the two competing localization schemes suggests that there is a resonance between these two localized solutions. These resonance structures reflect the delocalized nature of electronic density, a fact directly related to the aromaticity. The agreement between the MO and AdNDP pictures gives us confidence in using only the MO analysis in larger complexes where AdNDP is unfeasible. We additionally investigate the potential resonance structures of this molecule using natural resonance theory. We found five equivalent structures, where iridium is covalently bonded to three different hydrogens in each case, showing a high delocalization on the ring, something very characteristic of aromatic systems.

Nucleus-independent chemical shifts (NICSs)[34] are an often used aromaticity index, in spite of some recent debate on the issue.[35] Unfortunately, NICS(0) cannot be performed on this system, due to the presence of iridium at the geometric center of the ring, and NICS(1), NICS calculation 1 angstrom above the ring center, is meaningless due to the presence of d AOs of Ir and p AOs of phosphorous atoms.

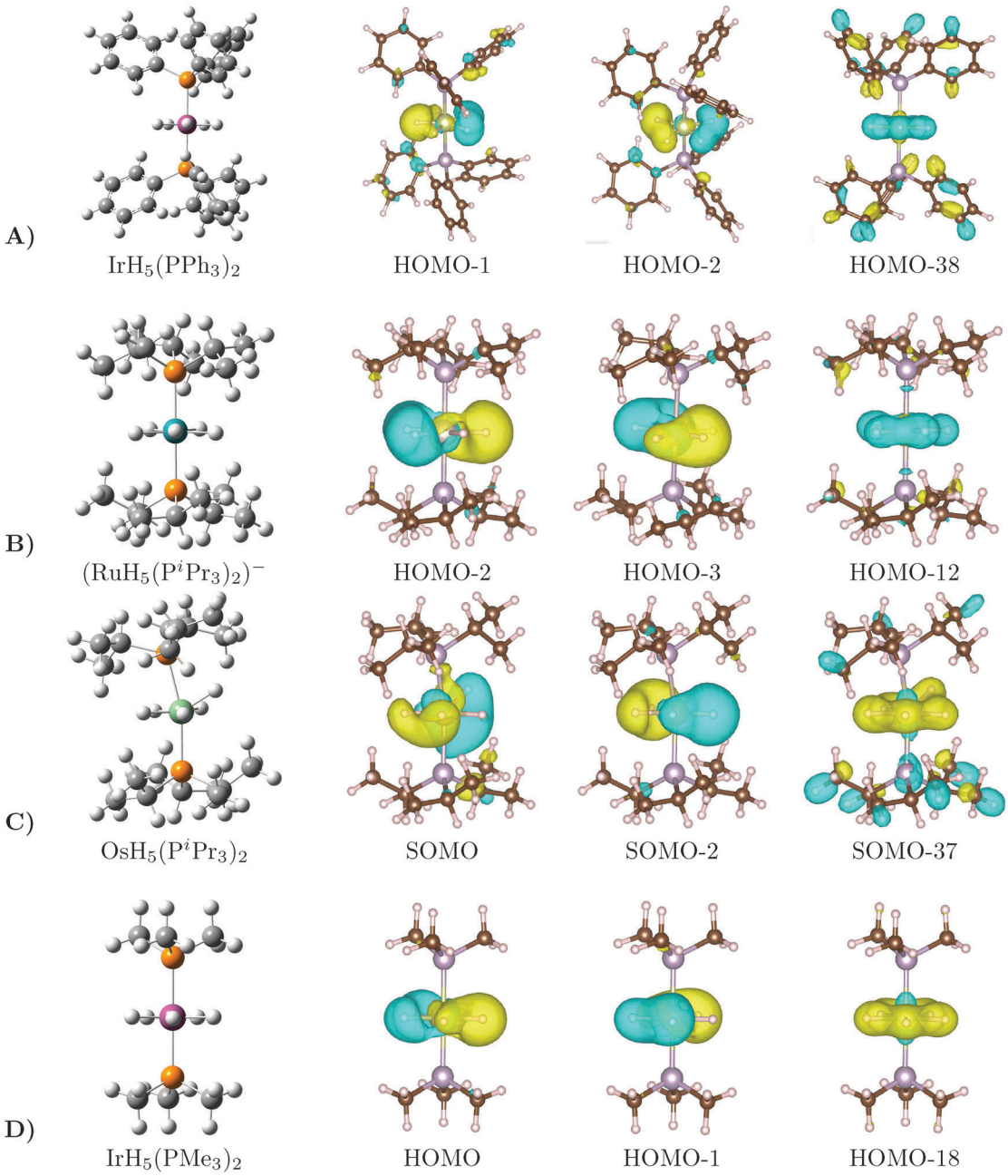

Fig. 1 Transition-metal hydride complexes along with the most relevant MOs in each case. The pink, turquoise, green, orange, gray and white spheres represent Ir, Ru, Os, P, C, and H atoms, respectively.

$(RuH_5(P^iPr_3)_2)^-$ and $(OsH_5(P^iPr_3)_2)^-$ molecules have the same singular arrangement as $IrH_5(PPh_3)_2$, where the transition-metal is coplanar to the 5 hydrogens to which it is bonded. The difference in this case is that the metal has two triisopropylphosphine ligands. $(RuH_5(P^iPr_3)_2)^-$ is shown in Fig. 1B, as representative since $(OsH_5(P^iPr_3)_2)^-$ has the same geometry. The analysis of the MOs reveals in both, ruthenium and osmium polyhydrides, exactly the same bonding picture. The most significant MOs of $(RuH_5(P^iPr_3)_2)^-$ are shown in Fig. 1B, while a more detailed picture can be found in the ESI.† The partially bonding HOMO−2 and HOMO−3 σ-MOs are mainly composed of the 1s AOs of hydrogens, with a contribution from the metal p AOs. Moreover, the HOMO−12 bonding σ-MO is formed by the 1s AOs of hydrogens mixed in some degree with the 1s AOs of the ruthenium atom. Note that the corresponding Os complex displays the same bonding picture. We characterized the neutral $OsH_5(P^iPr_3)_2$ and $RuH_5(P^iPr_3)_2$ complexes too, but they do not maintain the singular structure of their anions. Indeed, they have a Jahn–Teller distorted geometry. In Fig. 1C the $OsH_5(P^iPr_3)_2$ hydride is shown, where the P^iPr_3 ligands on the axial positions are moved from the linear angle and the hydrogens on the H_5 ring are not coplanar. The analysis of the

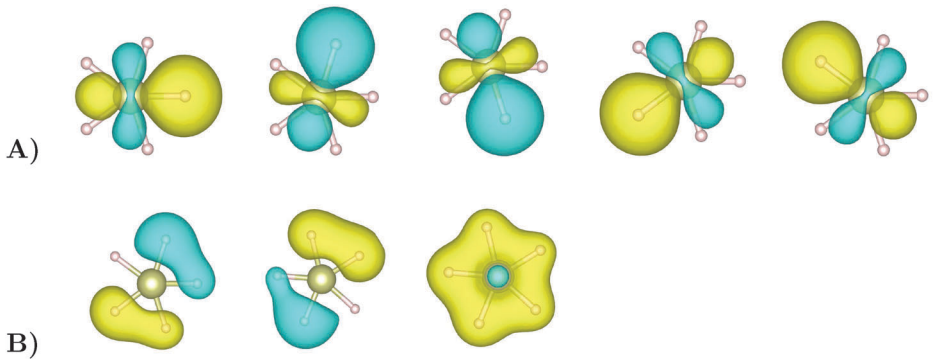

Fig. 2 The two different AdNDP bonding pictures for IrH_5.

MOs (Fig. 1C) shows that the singly occupied SOMO is one of the MOs formed by the five 1s AOs of the hydrogens, with a small contribution of osmium's 6p AO. The other 2 MOs where hydrogens are involved are preserved, although slightly distorted and quasi-degeneracy found in the previous more symmetric molecules is not retained, the energy difference between SOMO and SOMO−2 being *ca.* 25 kcal mol^{-1}. In other words, the delocalized system of σ-MOs is now populated by five electrons, leading to a Jahn–Teller situation. The same scene is found for $RuH_5(P^iPr_3)_2$. Thus the aromaticity argument can explain the geometric differences between these complexes. Note that the explanation would not be obvious if we would adopt the other localized AdNDP solution presented in Fig. 2A.

These molecules being aromatic, they should exhibit high stability. Often, transition-metal polyhydrides coordinate dihydrogen moieties.[36,37] Therefore, we decided to check whether $(IrH_5(PPh_3)_2)^{0,-1}$, $(RuH_5(P^iPr_3)_2)^-$, and $(OsH_5(P^iPr_3)_2)^-$ complexes would stabilize η^2-H_2 species. The result was meaningful: $(IrH_3(\eta^2\text{-}H_2)(PPh_3)_2)^{0,-1}$, $(IrH(\eta^2\text{-}H_2)_2(PPh_3)_2)^{0,-1}$, $(TMH_3(\eta^2\text{-}H_2)\text{-}(P^iPr_3)_2)^-$, and $(TMH(\eta^2\text{-}H_2)_2(P^iPr_3)_2)^-$ (where TM = Ru, Os) are not minima on the potential energy surfaces, as revealed by several imaginary frequencies. Instead, the optimization led us to the already characterized σ-aromatic structures, further confirming their large stability.

Now, would this σ-aromaticity be preserved with other transition-metals? And with different ligands? This would be interesting for experimentalists, since the electronic and steric effects could be tailored for particular applications or reactions. In fact metal phosphine complexes display good solubility in organic solvents, making them ideal for their use in homogeneous catalysis. In those cases, aromaticity contributes to stability and could ultimately affect the kinetics of the catalyzed reactions. To analyze this possibility, we characterized all the $(TMH_5L_2)^{0,-1}$ complexes, with TM = Ru, Os, Ir, and Pt and L = PMe_3, P^iPr_3, and PPh_3 for comparison. In Table 1 the charges of transition-metal and of hydrogens on the H_5 ring, along with the H–TM distances, are given for the resulting σ-aromatic structures. Undoubtedly iridium is the metal that better stabilizes this kind of structure: it forms σ-aromatic complexes with all the three ligands considered in this work. $IrH_5(PMe_3)_2$, for instance, is shown in Fig. 1D along with the MOs related to the σ-aromaticity. The only remarkable detail is

Table 1 Data corresponding to $(TMH_5L_2)^{0,-1}$ molecules: q_{TM} is the NBO charge of the transition-metal, q_H the NBO charge of the hydrogen atoms on the aromatic ring, and R(TM–H) the distance between the transition-metal and those hydrogen atoms in Å

	q_{TM}	q_H	R(TM–H)
$IrH_5(PMe_3)_2$	−1.88	0.12	1.63
$(IrH_5(PMe_3)_2)^-$	−2.12	0.07–0.09	1.64–1.65
$IrH_5(PPh_3)_2$	−1.80	0.12–0.14	1.63–1.64
$(IrH_5(PPh_3)_2)^-$	−1.80	0.09–0.11	1.64
$IrH_5(P^iPr_3)_2$	−1.92	0.11–0.12	1.63–1.64
$(IrH_5(P^iPr_3)_2)^-$ [a]	−1.89	0.08–0.12	1.63–1.64
$(RuH_5(PMe_3)_2)^-$	−2.75	0.13	1.66
$(RuH_5(PPh_3)_2)^-$	−2.69	0.13–0.15	1.64–1.66
$(RuH_5(P^iPr_3)_2)^-$	−2.71	0.12–0.13	1.65–1.66
$(OsH_5(PMe_3)_2)^-$	−2.31	0.06	1.68
$(OsH_5(PPh_3)_2)^-$	−2.21	0.06–0.08	1.66–1.67
$(OsH_5(P^iPr_3)_2)^-$	−2.28	0.06	1.67–1.69
$PtH_5(PMe_3)_2$	−1.24	0.08	1.62
$PtH_5(PPh_3)_2$	−1.25	0.09–0.10	1.62
$PtH_5(P^iPr_3)_2$	−1.23	0.07	1.61–1.62

[a] One C_3H_7 from one of the P^iPr_3 ligands is released.

that in the case of $(IrH_5(P^iPr_3)_2)^-$ one C_3H_7 from one of the P^iPr_3 ligands is released (ESI,† Fig. S4). But still the final molecule has the σ-aromatic arrangement. Along all the iridium polyhydrides the Ir–H distance is maintained constant. The charge on the metal atom is found to be the smallest when the ligand is PPh_3, this group being the least electron donating ligand. It is also notable that the calculated NBO charge on Ir is the same for the neutral and anionic $IrH_5(PPh_3)_2$ compound. In this case the excess of charge is located on the phenyl groups.

Osmium and ruthenium behave in a very similar way: both form anionic polyhydrides, regardless of the ligands. And all these anionic complexes are σ-aromatic, according to their bonding picture, obeying Hückel's electron counting rule. The corresponding neutral complexes, however, exhibit the previously mentioned Jahn–Teller distorted geometry. The NBO charges on both metals, shown in Table 1, are the smallest with triphenylphosphine ligands. The case of platinum, however, is radically different: neutral compounds are stable and σ-aromatic. The charges on Pt do not vary notably with different ligands. However, when considering the corresponding anionic polyhydrides,

we observed that during optimization the ligands on the axial positions released from the PtH_5 ring. The instability of these compounds can be understood taking into account that the 6s5d AOs of Pt are almost filled, and the addition of one extra electron effectively populated the antibonding orbital with the ligand that becomes unbound.

3.2 $OsH_4(PPhMe_2)_3$ and related compounds of Ir, Pt and Ru

$OsH_4(PPhMe_2)_3$ polyhydride is slightly different from the compounds described in the previous subsection, because the planar pentagonal ring is composed of 4 hydrogens and a phosphorous atom from one of the ligands, with the transition-metal located at the center of this ring, see Fig. 3A. On the axial positions the compound has two dimethylphenylphosphine, moved from the linear angle, due to the steric repulsion created by the PMe_2Ph fragment on the ring. The MOs formed by hydrogens' AOs are shown in Fig. 3A (the full set of valence MOs can be found in the ESI†). The bonding picture is similar to the one found in the $IrH_5(PPh_3)_2$ molecule, even though one of the positions on the 5-membered ring is now taken by the phosphorous atom. The HOMO−3 is formed by the 1s AO of hydrogens and a small contribution coming from the p orbital of osmium. The HOMO−5 MO, however, is composed not only of the 1s-AO of hydrogens but also of the 3p-AO of the phosphorous atom in the ring and the 6p-AO of Os. It should be noted that this MO exhibits a slight further delocalization of the electron density,

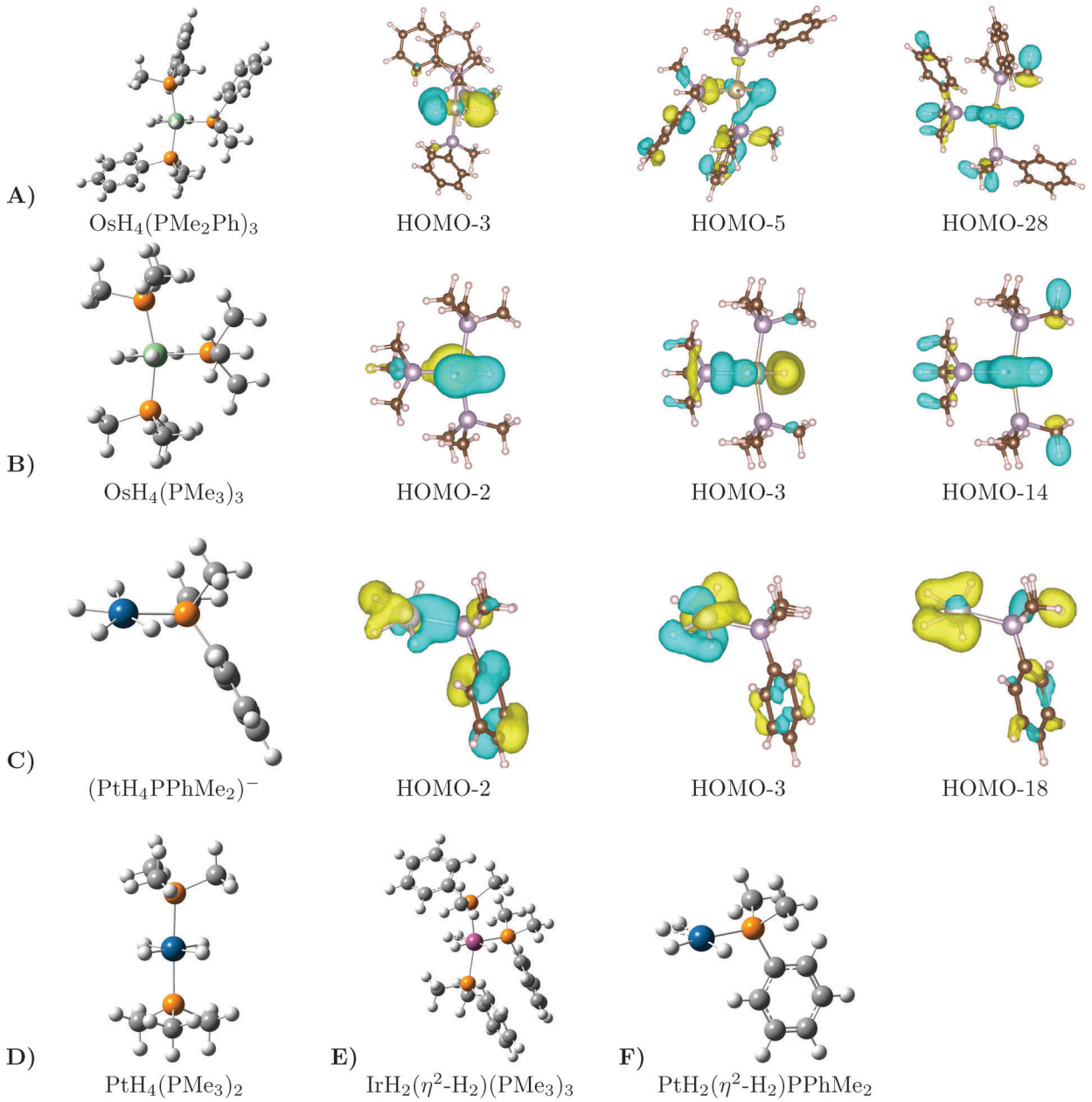

Fig. 3 Transition-metal hydride complexes. The pink, green, blue orange, gray and white spheres represent Ir, Os, Pt, P, C, and H atoms, respectively.

Table 2 Data corresponding to $(TMH_4L_3)^{0,-1}$ molecules: q_{TM} is the NBO charge of the transition-metal, q_H the NBO charge of the hydrogen atoms on the aromatic ring, and R(TM–H) the distance between the transition-metal and those hydrogen atoms in Å

	q_{TM}	q_H	R(TM–H)
$OsH_4(PMe_3)_3$	−2.17	0.09–0.14	1.65–1.68
$(OsH_4(PMe_3)_3)^-$	−2.28	0.09–0.13	1.65–1.68
$OsH_4(PMe_2Ph)_3$	−2.10	0.06–0.17	1.65–1.69
$(OsH_4(PMe_2Ph)_3)^-$	−2.10	0.07–0.14	1.64–1.68
$RuH_4(PMe_3)_3$	−2.69	0.15–0.24	1.62–1.66
$RuH_4(PMe_2Ph)_3$	−2.64	0.13–0.27	1.61–1.66
$(RuH_4(PMe_2Ph)_3)^-$	−2.61	0.14–0.22	1.61–1.66

over the benzene substituent of the ligand in the ring and the second benzene on one of the axial ligands. Finally, the HOMO−28 MO is mainly composed of hydrogens' 1s-AOs and the 3s-AO of the phosphorous atom on the ring with a stabilizing contribution of the Os 6s-AO. Despite the lack of precise symmetry, this compound can be classified as σ-aromatic according to Hückel's electron counting rule ($4n + 2$ with $n = 1$). Furthermore, it should be noted that the $(OsH_4(PPhMe_2)_3)^-$ anion is stable and has the same σ-aromatic arrangement as its neutral counterpart.

The natural resonance theory shows different resonance structures, where the covalent bonds between osmium, hydrogens and the phosphorous atom participating in the σ-aromatic ring are swapped. The weight of these resonance structures varies from about 10% to 5%, due to the lack of symmetry of the molecule.

In order to check the stability of the neutral and anionic $OsH_4(PPhMe_2)_3$ molecules against the formation of η^2-H_2 species, we calculated the structures with either one or two η^2-H_2 moieties, but none of them were stable, as it was found with the transition-metal polyhydrides in the previous Section 3.1, highlighting the large stability of the σ-aromatic hydride complexes.

Once σ-aromaticity is proved in this hydride complex, we optimized the $OsH_4(PMe_3)_3$ molecule, shown in Fig. 3B and confirmed not only that it is stable, but also that it has the same σ-aromatic bonding pattern in the ring (see Fig. 3B). It is worth noting that the $(OsH_4(PMe_3)_3)^-$ anion is also stable and possesses the same σ-aromatic arrangement. The calculated NBO charges on osmium and hydrogens on the ring are shown in Table 2, along with the Os–H distances, for the several aromatic molecules. Note that charges on H atoms are different because of the lack of symmetry in the molecule due to the presence of one ligand on the ring. Overall the results are very similar to those for $(OsH_4(PPhMe_2)_3)^{0,-1}$. Thus, the substitution of the phenyl by a methyl group will be used to modify the steric effects of the molecule, while preserving the similar electronic features.

Additionally, we have investigated if ruthenium, iridium and platinum atoms could benefit from the σ-aromaticity and form similar compounds. Ru indeed forms this kind of aromatic polyhydrides, with both $PPhMe_2$ and PMe_3 ligands. The only exception is $(RuH_4(PPhMe_2)_3)^-$, which is unstable due to the release of the ligand on the ring. In fact, the calculated NBO charges reveal that ruthenium has a bigger negative charge than osmium in all the studied compounds, and this charge is even bigger when the ligand is trimethylphosphine, due to its greater electron donating nature. Thus, the negatively charged $(RuH_4(PMe_3)_3)^-$ is found to be unstable.

Regarding Ir and Pt, unfortunately, they do not form stable neutral or anionic $TMH_4(PMe_3)_3$ polyhydres, since the PMe_3 on the ring releases from these molecules, leading to the $TMH_4(PMe_3)_2$ complexes shown in Fig. 3D. This again can be attributed to the excess number of electrons in these attempted species. Nevertheless, the study of potentially aromatic $TMH_4(PPhMe_2)_3$ structures led us to some stimulating structures. For iridium complexes, $IrH_4(PPhMe_2)_3$ was found not to retain the planar-pentagonal coordination for the metal. Instead, a non-aromatic molecule was formed, where two of the hydrogen atoms formed a metal-coordinated H_2 molecule with a bond-length of 0.88 Å, see Fig. 3E. Thus, this interesting complex should be called $IrH_2(\eta^2\text{-}H_2)(PPhMe_2)_3$ and could have a wide range of applications in catalysis or organic synthesis. Its anionic form, however, is not stable due to the release of $PPhMe_2$ belonging to the ring.

In regard to platinum, both neutral and anionic $PtH_4(PPhMe_2)_3$ are found to be unstable, because the ligands on the axial positions are separated from the PtH_4PPhMe_2 moiety, as could be expected taking into account the fact that its 6s5d AO's are almost filled. Nonetheless, we were able to characterize the $(PtH_4PPhMe_2)^{0,-1}$ hydride complexes. On the one hand, the optimization of the neutral compound gave rise to the structure shown in Fig. 3F, where the η^2-H_2 fragment can be easily identified. The H–H bond length is 0.85 Å. The NBO charges on hydrogens are close to 0 (from −0.08 to 0.10) and the charge on Pt is −0.46, substantially smaller compared to the rest of metallic polyhydrides studied in this work. On the other hand, the anionic $(PtH_4PPhMe_2)^-$ polyhydride (see Fig. 3C), with an open-shell electronic structure, is not completely planar due to the Jahn–Teller distortion, although the σ-aromaticity is preserved (see Fig. 3C).

3.3 $PtZnH_5^-$, $IrZnH_5^-$, $OsZnH_5^-$ and $RuZnH_5^-$

Taking into account that both osmium and iridium are able to have a pentagonal planar coordination, stabilized through σ-aromaticity, it is likely that they would also form a similar structure to that of the $PtZnH_5^-$ cluster. Therefore, in the last part of this work we studied the $TMZnH_5^-$ hydride complexes, where TM = Pt, Ru, Os and Ir. Since Pt, Ru and Os complexes display the same behavior, we will focus in this section on the description of iridium and osmium polyhydrides. Both molecules are shown in Fig. 4. The NBO charges and TM–H distances presented in Table 3 show that Ru has the bigger charge, and when going from Os to Pt the charges decrease, the bond lengths between TM and the hydrogens shrink, as expected, while the hydrogen atoms are almost neutral. The MOs where hydrogens are involved are shown in Fig. 4A and B for $IrZnH_5^-$ and $OsZnH_5^-$, respectively (more details can be found in the ESI†). Observe that these MOs are very similar to those of the previously analyzed hydride complexes. The first two σ-MOs are partially bonding. The HOMO−6 in $IrZnH_5^-$ and HOMO−7 in $OsZnH_5^-$

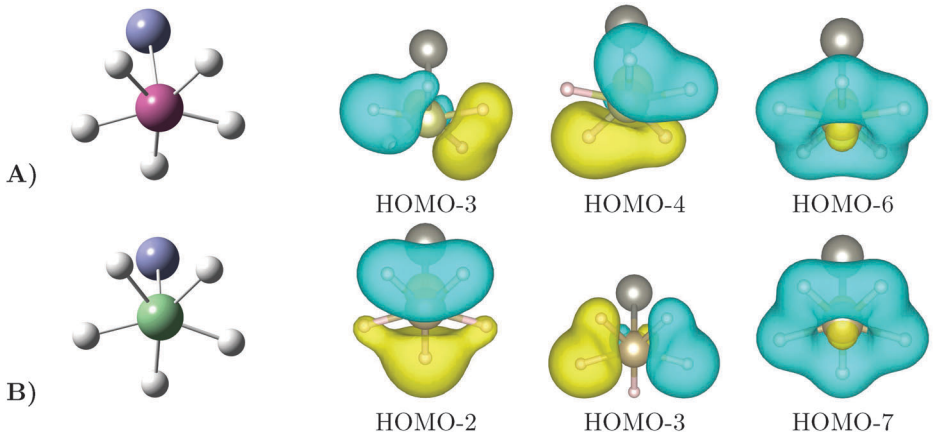

Fig. 4 Anionic $TMZnH_5^-$ polyhydride complexes. (A) $IrZnH_5^-$ molecule along with the most relevant MOs of $IrZnH_5^-$ and (B) $OsZnH_5^-$ molecule and its most relevant MOs of $OsZnH_5^-$ are shown. Ir, Os, Zn and H are represented with pink, green, violet and white spheres, respectively.

Table 3 Data corresponding to $(TMH_5Zn)^{0,-1}$ molecules: q_{TM} is the NBO charge of the transition-metal, q_H the NBO charge of the hydrogen atoms on the aromatic ring, and R(TM–H) the distance between the transition-metal and those hydrogen atoms in Å

	q_{TM}	q_H	R(TM–H)
$(RuH_5Zn)^-$	−1.64	0.02	1.65
$(OsH_5Zn)^-$	−1.53	−0.02	1.67
$(IrH_5Zn)^-$	−1.45	<0.01	1.64
IrH_5Zn	−1.14	−0.02–0.08	1.67–1.61
$(PtH_5Zn)^-$	−1.17	0.01	1.62

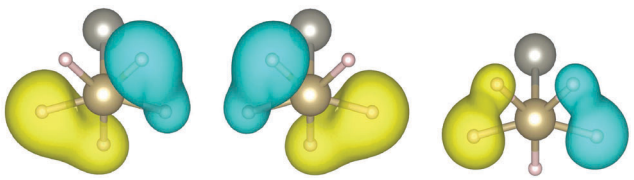

Fig. 5 AdNDP result for the $OsZnH_5^-$ complex.

are completely bonding. Thus, populated with 6 electrons, these molecules fulfill Hückel's electron counting rule ($4n + 2$ with $n = 1$), and they are σ-aromatic. Also, as in the previous cases, the presence of the TM is essential for the support of this bonding feature.

To further analyze the bonding in these molecules, we took advantage of the small size of these compounds and performed an AdNDP analysis on the $OsZnH_5^-$ cluster. Note that AdNDP analysis cannot be performed on $IrZnH_5^-$ because it is has a doublet open-shell electronic structure. Lone pairs of osmium, with population numbers as big as 1.45, were found and removed from the density matrix. AdNDP then localized one 2c–2e between Os and Zn and three 6c–2e involving the aromatic ring, see Fig. 5. This analysis thus confirms σ-aromaticity in the systems. The potential resonance structures of this molecule were determined using natural resonance theory. For both $OsZnH_5^-$ and $IrZnH_5^-$ five equivalent resonance structures were found. In each structure there are two pairs of hydrogens covalently bonded, while the fifth hydrogen is covalently bonded to Os (Ir). This fact reflects the delocalization of the electronic density related to the σ-aromaticity.

Finally, we also characterized the neutral $TMZnH_5$ polyhydrides, shown in Fig. 6A–C. The σ-aromaticity is only preserved in the $IrZnH_5$ complex (see Fig. 6A), even though Zn is moved from the linear position in the anionic compound. Both $OsZnH_5$

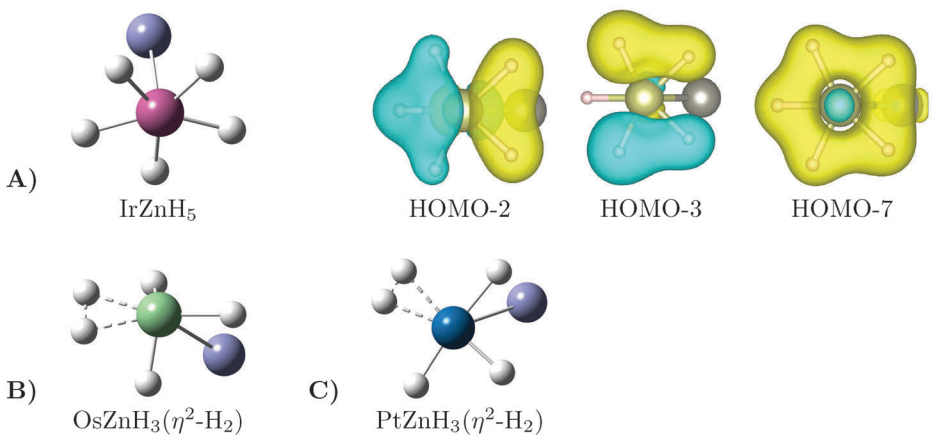

Fig. 6 Neutral $TMZnH_5$ polyhydrides. (A) $IrZnH_5$ along with the most relevant MOs of $IrZnH_5$, (B) $OsZnH_5$ and (C) $PtZnH_5$ are shown. Pt, Ir, Os, Zn, and H are represented with blue, pink, green, violet and white spheres, respectively.

and $PtZnH_5$, having open-shell electronic structures, are highly distorted due to the first order Jahn–Teller effect. As a consequence, the hydrogens do not retain the planar-pentagonal coordination for TM and two of the hydrogen atoms form a metal-coordinated H_2 molecule, with H–H bond-lengths of 0.92 Å in $OsZnH_3(\eta^2\text{-}H_2)$ and 0.86 Å in $PtZnH_3(\eta^2\text{-}H_2)$.

4 Conclusions

Transition-metal hydrides represent a unique class of compounds which are essential for catalysis, organic synthesis and hydrogen storage. Aromaticity explains the stabilization of a chemical system in symmetric geometry due to the specific count of electrons in a set or sets of delocalized MOs; it is associated with special stability and reduced and/or specific reactivity, and thus is important to realize in the studied compounds. The recent joint experimental and theoretical work studied the $PtZnH_5^-$ cluster anion, where the singular planar pentagonal pyramidal coordination for platinum was found to be due to the σ-aromaticity of the H_5 cycle. This led us to the investigation of four already synthesized polyhydrides: $IrH_5(PPh_3)_2$, $(RuH_5(P^iPr_3)_2)^-$, $(OsH_5(P^iPr_3)_2)^-$, and $OsH_4(PPhMe_2)_3$. The distinctive feature of these molecules is that, like in the $PtZnH_5^-$ cluster, the metal has a five coordinated arrangement in-plane, along with additional ligands at the axial positions. This work shows that this exceptional geometrical arrangement is indeed possible thanks to the σ-aromaticity. Accordingly, the species considered in this work not only have uncommon structural and electronic properties, but are also highly stable. Based on these findings, we further proposed a new family of polyhydrides of Ir, Ru, Os, and Pt that display a uniquely 5-fold coordination in plane. These molecules might have important applications in different fields of chemistry, such as organic synthesis and catalysis. Additionally, this work led to some particular metallic complex hydrides, with an activated metal-coordinated $\eta^2\text{-}H_2$ fragment that might be useful in catalysis applications.

Therefore, overall these transition-metal polyhydrides can be classified into two groups: aromatic and non-aromatic systems. The aromatic molecules are highly symmetric, showing an unusual planar pentagonal coordination of the metal. They are highly stable and, in fact, for these compounds the coordination to the $\eta^2\text{-}H_2$ moiety is unfavorable, indicating that a bound dihydrogen would undergo dissociation in favor of acquired σ-aromaticity. The non-aromatic molecules, conversely, have a distorted geometry, showing Jahn–Teller distorsion or dihydrogen bonds. Some of them also tend to merely activate, and not split the H–H bond in the H_2 molecule. Thus, from a simple electron count, one can rationalize their structures and make predictions about their reactivity.

Acknowledgements

The authors acknowledge support from the Air Force Office of Scientific Research under AFOSR BRI Grant FA9550-12-1-0481, and the NSF CAREER Award CHE1351968. Computational resources were provided by the UCLA-IDRE cluster.

References

1 A. I. Boldyrev and L. Wang, *Chem. Rev.*, 2005, **105**, 3716–3757.
2 A. N. Alexandrova, A. I. Boldyrev, H.-J. Zhai and L.-S. Wang, *Coord. Chem. Rev.*, 2006, **250**, 2811–2866.
3 T. R. Galeev and A. I. Boldyrev, *Annu. Rep. Prog. Chem., Sect. C: Phys. Chem.*, 2011, **107**, 124–147.
4 D. Y. Zubarev, B. B. Averkiev, H. Zhai, L. Wang and A. I. Boldyrev, *Phys. Chem. Chem. Phys.*, 2008, **10**, 257–267.
5 A. N. Alexandrova and A. I. Boldyrev, *J. Phys. Chem. A*, 2003, **107**, 554–560.
6 F. Feixas, E. Matito, J. Poater and M. Solá, *Wiley Interdiscip. Rev.: Comput. Mol. Sci.*, 2013, **3**, 105–122.
7 P. K. Chattaraj, *Aromaticity and Metal Clusters*, Taylor & Francis, CRC Press, Boca Raton, 2011.
8 C. A. Tsipis, *Coord. Chem. Rev.*, 2005, **249**, 2740–2762.
9 R. W. A. Havenith, F. D. Proft, P. W. Fowler and P. Geerlings, *Chem. Phys. Lett.*, 2005, **407**, 391–396.
10 H. Jiao, P. R. Schleyer and M. N. Glukhovtsev, *J. Phys. Chem.*, 1996, **100**, 12299–12304.
11 X. Zhang, G. Liu, G. Gantefoer, K. H. Bowen and A. N. Alexandrova, *J. Phys. Chem. Lett.*, 2014, **5**, 1596–1601.
12 M. A. Esteruelas, F. J. Fernández-Alvarez, M. Oliván and E. Oñate, *Organometallics*, 2009, **28**, 2276–2284.
13 S. E. Clapham and R. H. Morris, *Organometallics*, 2005, **24**, 479–481.
14 S. Fukuzumi, *Eur. J. Inorg. Chem.*, 2008, 1351–1362.
15 Z. M. Heiden and T. B. Rauchfuss, *J. Am. Chem. Soc.*, 2007, **129**, 14303–14310.
16 A. Fabrello, A. Bachelier, M. Urrutigoity and P. Kalck, *Coord. Chem. Rev.*, 2010, **254**, 273–287.
17 F. Maseras, A. L. E. Clot and O. Eisenstein, *Chem. Rev.*, 2000, **100**, 601–636.
18 G. G. Hlatky and R. H. Crabtree, *Coord. Chem. Rev.*, 1985, **65**, 1–48.
19 M. Loza, J. W. Faller and R. H. Crabtree, *Inorg. Chem.*, 1995, **34**, 2937–2941.
20 K. Abdur-Rashid, D. G. Gusev, A. J. Lough and R. H. Morris, *Organometallics*, 2000, **19**, 834–843.
21 K. Abdur-Rashid, D. G. Gusev, S. E. Landau, A. J. Lough and R. H. Morris, *J. Am. Chem. Soc.*, 1998, **120**, 11826–11827.
22 P. G. Douglas and B. L. Shaw, *J. Chem. Soc. A*, 1970, 334–338.
23 J. P. Perdew, K. Burke and M. Ernzerhof, *Phys. Rev. Lett.*, 1997, **78**, 1396.
24 J. P. Perdew, K. Burke and M. Ernzerhof, *Phys. Rev. Lett.*, 1996, **77**, 3865–3868.
25 C. Adamo and V. Barone, *J. Chem. Phys.*, 1999, **110**, 6158–6170.
26 W. Kohn and L. J. Sham, *Phys. Rev.*, 1965, **140**, A1133.
27 P. Hohenberg and W. Kohn, *Phys. Rev.*, 1964, **136**, B864.
28 M. J. Frisch, G. W. Trucks, H. B. Schlegel, G. E. Scuseria, M. A. Robb, J. R. Cheeseman, G. Scalmani, V. Barone, B. Mennucci, G. A. Petersson, H. Nakatsuji, M. Caricato, X. Li, H. P. Hratchian, A. F. Izmaylov, J. Bloino, G. Zheng, J. L. Sonnenberg, M. Hada, M. Ehara, K. Toyota, R. Fukuda,

J. Hasegawa, M. Ishida, T. Nakajima, Y. Honda, O. Kitao, H. Nakai, T. Vreven, J. A. Montgomery, Jr., J. E. Peralta, F. Ogliaro, M. Bearpark, J. J. Heyd, E. Brothers, K. N. Kudin, V. N. Staroverov, R. Kobayashi, J. Normand, K. Raghavachari, A. Rendell, J. C. Burant, S. S. Iyengar, J. Tomasi, M. Cossi, N. Rega, J. M. Millam, M. Klene, J. E. Knox, J. B. Cross, V. Bakken, C. Adamo, J. Jaramillo, R. Gomperts, R. E. Stratmann, O. Yazyev, A. J. Austin, R. Cammi, C. Pomelli, J. W. Ochterski, R. L. Martin, K. Morokuma, V. G. Zakrzewski, G. A. Voth, P. Salvador, J. J. Dannenberg, S. Dapprich, A. D. Daniels, O. Farkas, J. B. Foresman, J. V. Ortiz, J. Cioslowski and D. J. Fox, 2009.

29 F. Weigend and R. Ahlrichs, *Phys. Chem. Chem. Phys.*, 2005, **7**, 3297–3305.

30 E. D. Glendening, A. E. Reed, J. E. Carpenter and F. Weinhold, NBO Version, 2013.

31 E. D. Glendening and F. Weinhold, *J. Comput. Chem.*, 1998, **19**, 593–609.

32 E. D. Glendening, J. K. Badenhoop and F. Weinhold, *J. Comput. Chem.*, 1998, **19**, 628–646.

33 D. Y. Zubarev and A. I. Boldyrev, *Phys. Chem. Chem. Phys.*, 2008, **10**, 5207–5217.

34 P. v. R. Schleyer, C. Maerker, A. Dransfeld, H. Jiao and N. J. v. E. Hommes, *J. Am. Chem. Soc.*, 1996, **118**, 6317.

35 C. Foroutan-Nejad, *Theor. Chem. Acc.*, 2015, **134**, 8–16.

36 G. S. Mcgrady and G. Guilera, *Chem. Soc. Rev.*, 2003, **32**, 383–392.

37 L. Andrews, *Chem. Soc. Rev.*, 2004, **33**, 123–132.